J. Geophys. 44, 545–555 1978

Journal of Geophysics

Palaeosecular Variation Studies of the Brunhes Epoch in the Volcanic Province of the East-Eifel, Germany

H. Kohnen and H. Westkämper

Institut für Geophysik der Universität Münster,
Gievenbecker Weg 61, 4400 Münster, Federal Republic of Germany

Abstract. In the Quarternary volcanic province of the East-Eifel 46 occurrences were investigated palaeomagnetically. According to radiometric dating, the volcanic activity covered the past 600,000 years more or less uniformly and is adequate to study the palaeosecular variation of the Brunhes epoch. The mean pole position (VGP) of the occurrences investigated follow a Fisherian distribution. Averaging all pole positions yields 87.0° N and 69.2° E ($A_{95}=4.8°$) which coincides with the north geographic pole within the limits of error. This agreement shows that the area as well as the time interval are large enough in this particular case to confirm the axial dipole hypothesis. The angular dispersion of the VGP: $S_F=15.1°$ (angular dispersion of the ancient field) is in accordance with the models C, E, and M proposed for the palaeosecular variation of the earth's magnetic field.

Key words: Palaeomagnetic investigations – Quartenary volcanics of the East-Eifel – Palaeosecular variation – Mean pole position – Angular dispersion.

Introduction

The East-Eifel is part of the Rhenian Mass (Rheinisches Schiefergebirge), which consists mainly of quartzites, gray-wakes and slates of the Lower Devonian. The area of young volcanism extends between the rivers Rhine (N, NE), Nette (S, SW) and Brohl (N, NW) (Fig. 1). The onset of the volcanic activity coincided roughly with the beginning of the Pleistocene glaciation.

About 70 volcanic occurrences are known in this volcanic province of which 46 sites were palaeomagnetically investigated during 1976/77. The ages of several sites based on radiometric and stratigraphic dating, are listed in Figure 2. The dominating rock types are alkali basalts and among these mainly basanites, nephelinites, tephrites and phonolites. The time interval of the whole cycle seemed adequate to study the palaeosecular variation of the Brunhes epoch in this region.

0340-062X/78/0044/0545/$02.20

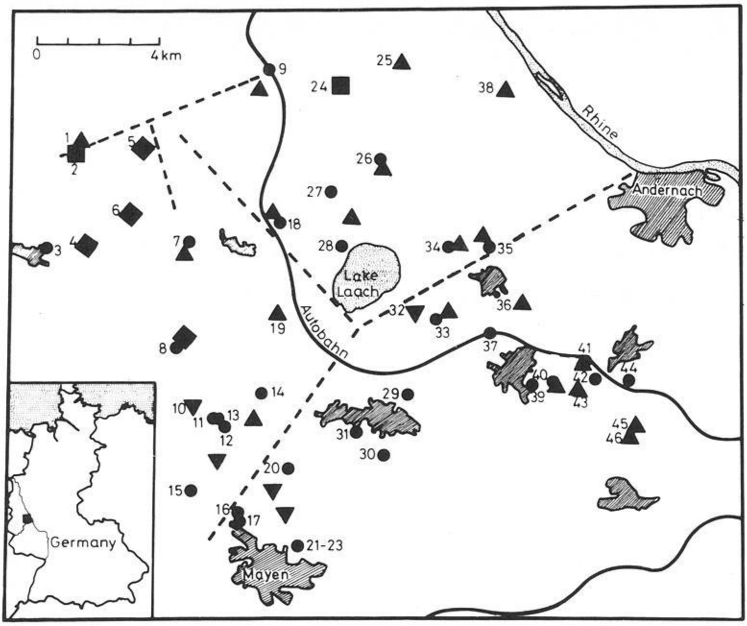

Fig. 1. Sampling sites in the East Eifel. The angular symbols denote volcanoes which are petrologically investigated. ▲ basanite; ■ nephelinite; ◆ phonolite; ▼ tephrite; the circles indicate additional localities investigated palaeomagnetically during this study. ------ Plio-Pleistocene faults

Of principal interest herein is a comparison of the palaeosecular variation of the Pleistocene or the Brunhes epoch respectively in the East-Eifel with the global palaeosecular variation.

The Models of Palaeosecular Variation

Different models based on historical observations of the geomagnetic field and on theoretical considerations have been developed to describe the global pattern and behaviour of the palaeosecular variation. Any latitudinal dependence of the palaeosecular variation should be manifest in the angular dispersion of the pole positions, which, therefore, is the quantity of basic importance in all models. The principles of the models developed so far are briefly outlined below and presented in Figure 3.

According to model A (Irving and Ward, 1964), the palaeosecular variation is only due to a non-dipole component of random direction but constant intensity. Model B (Creer et al., 1959) postulates a wobble of the main dipole following a Fisherian distribution. Such a latitudinal invariance of the angular standard deviation of the VGPs is not at all confirmed by experimental data. In Model C (Cox, 1962; Creer, 1962), the total angular dispersion is assumed to be a superposition of angular dispersions, due to a dipole wobble (S_D^2) and non-dipole components (S_N^2): $S_T^2 = S_D^2 + S_N^2$.

2 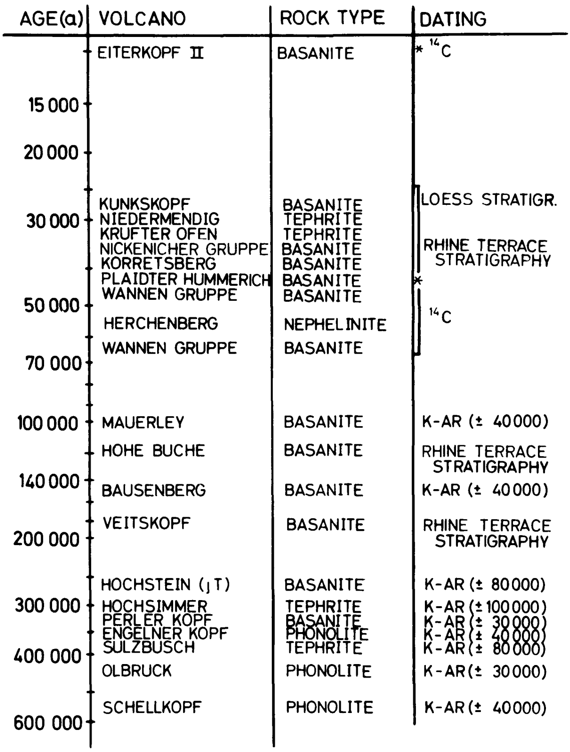

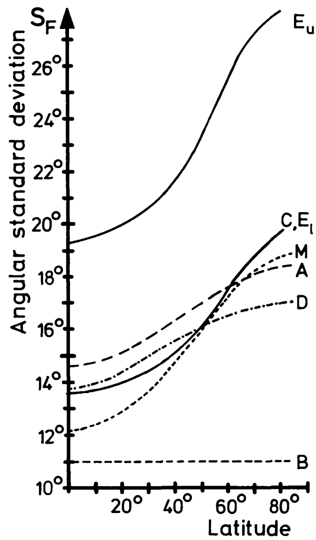 3

Fig. 2. Radiometric and stratigraphic ages of several quarternary volcanics in the Eifel after Frechen (1976) and *Schmincke (pers. communication).

Fig. 3. Different models proposed for the palaeosecular variation: A (Irving and Ward, 1964); B (Creer et al., 1959); C (Cox, 1962; Creer, 1962); D (Cox, 1970); E (Baag and Helsley, 1974a); E_u: upper limit of model E with $r=1$; E_1: lower limit of model E with $r=0$); and M (McElhinny and Merrill, 1975). See text for explanation

S_N is deduced by using averaged data from the 1965 International Geomagnetic Reference Field. $S_D=11°$ is based on palaeomagnetic measurements on the Hawaiian lavas, where non-dipole components are supposed to be absent (Pacific dipole window). Model D (Cox, 1970) is principally similar to model C; S_N, however, is based on theoretical assumptions. In model E (Baag and Helsley, 1974a), a linear coupling between S_D and S_N is proposed: $S_T^2=S_D^2+S_N^2+2r\,S_D S_N$ $(0 \leqq r \leqq 1)$. The values for S_D and S_N are taken from model C. C and E are consequently identical for $r=0$. Model M (McElhinny and Merrill, 1975) is an extension of model D. However, McElhinny, and Merrill propose a non-dipole field consisting of two components due to different mechanisms in the earth's interior. The intensity of the first component is invariant with latitude whereas the intensity of the second component increases with increasing latitude like the intensity of the dipole field. This separation is in accord with the investigations of Yukutake and Tachinaka (1969) splitting the non-dipole field in a standing and drifting part of similar magnitude. Curve M is calculated from:

$$S_T^2 = S_D^2 + (a W_{DP}^2 + b W_{NF}^2) S_N^2.$$

W_{NF} and W_{DP} are terms describing the latitudinal dependence of the components of the non-dipole field. $S_D = 9°$, $S_N = 8.25°$ (non-dipole component at the equator), $a = 0.25$ and $b = 0.75$ $(a + b = 1)$ are taken by the authors to obtain a best model fit to the present as well as to the past non-dipole field.

All models tacitly anticipate an axial geocentric dipole. The time average of VGPs spanning a period, which is large compared with the secular cycles of the geomagnetic field, should consequently yield coincidence between the dipole and the rotational axis. However, a critical review (McElhinny and Merrill, 1975) of all palaeosecular investigations of volcanics younger than two million years shows that 45% of the VGPs give significant differences between the geomagnetic and geographic north pole.

Only comprising various investigation areas of equal latitude yields satisfactory results. Some of the differences may be due to the two sources of the non-dipole field as outlined by Yukutake and Tachinaka (1969). If the magnetic field in the investigation area is mainly controlled by a great standing part, time averaging over long periods might not cancel out the differences entirely. McElhinny and Merrill (1975) argue, that for some areas the period of the volcanic activity might have not been long enough or insufficiently covered with regard to volcanic productivity. The latter point is particularly important because there seem to be cycles of secular variation of about 200,000 years (McElhinny and Merrill, 1975). Thus, the crucial problem also in the present study is, whether the investigation area of only $20 \times 24\ \mathrm{km}^2$ is large enough or the time period of approx. 600,000 years is long enough to fulfil the requirements outlined by McElhinny and Merrill (1975).

Field and Laboratory Procedure

Figure 1 shows the sites investigated palaeomagnetically during 1976 and 1977. The angular symbols denote volcanics with wellknown petrological nature. The circles represent localities, whose relation to distinct centres of eruption are somewhat speculative. From each site, 6 to 17 cores each giving 2 or 3 specimens were taken. A fluxgate spinner magnetometer (Digico) was used to determine intensity and direction of the magnetization of the specimens. The stability of the natural remanent magnetization (NRM) was tested by demagnetizing 2 to 3 pilot specimens from each site in alternating fields up to 56,000 A/m (1 OE $\hat{=}$ 80 A/m). Figure 4 presents typical demagnetization curves, the normalized intensities being plotted against the peak alternating fields. The stability against demagnetization increases from curve A to D. Curve A represents a magnetically unstable, coarse-grained phonolite from a lava flow. The maximum may be caused by ambient fields acting opposite to the direction of the NRM during storage. Some of the samples were able to acquire considerable secondary viscous components when stored for days or weeks in the earth's magnetic field or when subjected for a short time to small artificial fields as will be shown elsewhere (Böhnel and Kohnen, in

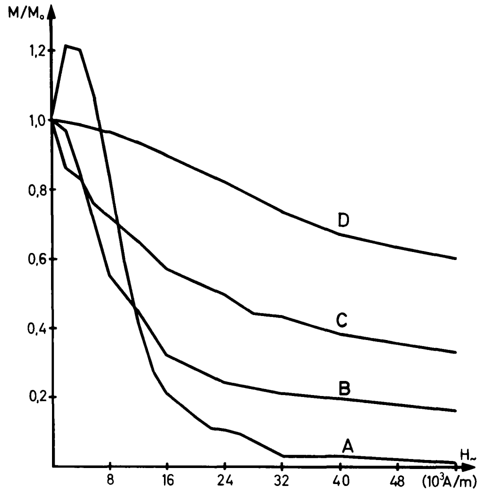

Fig. 4. Normalized NRM intensity versus peak alternating field.
A Phonolite (Olbrück, EEL 5),
B Nephelinite (Herchenberg, EEL 24),
C Basanite (Meirother Kopf, EEL 7),
D Tephrite (Krufter Ofen, EEL 32)

preparation). Curve D is obtained from a fine-grained volcanic scoria. Most results range in between the curves B and C. The differences between the extremes can be attributed to the grain size variation and are not a characteristic feature of the rock types encountered (Böhnel and Kohnen, in preparation). Most of the viscous magnetization was erased in alternating fields of only 8,000 A/m to 16,000 A/m. The directional stability of the remanent magnetization of the pilot specimens was estimated applying the stability index of Symons and Stupavsky (1974): PSI $=|d\mathbf{r}(H)/dH|$ ($\mathbf{r}$ = unit vector of magnetization; H = demagnetizing field). PSI should be zero in the most stable region but minimum values are usually obtained. All other specimens were then demagnetized in alternating fields covering this region. The site mean direction of the characteristic remanent magnetization (CARM) was taken from the stable region at alternating fields yielding minimum α_{95} angles of confidence. Best results were obtained at fields between 8,000 and 24,000 A/m.

Results

1. The Mean Pole Positions (VGP)

Taking into account the above selection criteria, the site mean directions, the pole positions and the precision parameters were calculated from the core means. The results are listed in Table 1.

There is considerable geological and geomorphological evidence that some of the sites investigated result from the same volcanic event. Additional proof was obtained from the site mean directions being identical within the limits of statistical error (F-test). These sites were consequently combined and their relevant results averaged as indicated in Table 1 resulting in 31 independent volcanic events.

Table 1. Summary of palaeomagnetic results from the Pleistocene volcanics of the East-Eifel province. N_0.: site number; n: number of cores; M_0: intensity of the natural remanent magnetization (NRM); H: peak alternating field at which the site mean direction of the characteristic remanent magnetization (CARM) is taken; *Dec*, *Inc*: site mean direction of the CARM; R: resultant vector; k: precision parameter; s: standard deviation of the within-site angular dispersion; *Long*, *Lat*: position of the virtual geomagnetic poles; dp, dm: parameters of the 95% ovals of confidence

N_0	n	M_0 (A/m)	H (A/m)	*Dec* (°)	*Inc* (°)	R	k	s (°)	d_{95} (°)	*Long* (°)	*Lat* (°)	dp (°)	dm (°)
EEL 1	6	0.650	12,000	28.8	70.3	5.99106	559	3.4	2.8	73.0	72.1	4.2	4.9
EEL 2	12	2.919	16,000	31.8	64.8	11.84619	72	9.6	5.2	94.7	68.8	6.7	8.3
EEL 3	6	0.118	8,000	10.3	71.8	5.98846	433	3.9	3.2	47.7	81.3	5.0	5.7
EEL 4	8	0.157	32,000	20.5	66.6	7.97692	303	4.7	3.2	94.7	76.8	4.3	5.2
EEL 5	6	0.090	16,000	72.3	81.5	5.96908	162	6.4	5.3	33.9	52.6	9.9	10.2
EEL 6	10	0.242	4,000	37.0	75.6	9.90526	95	8.3	5.0	51.1	66.6	8.4	9.2
EEL 7	7	5.048	28,000	0.5	63.7	6.98189	331	4.5	3.3	183.7	84.9	4.2	5.3
EEL 8	10	0.126	6,000	5.3	60.6	9.93968	149	6.6	4.0	162.7	80.4	4.6	6.0
EEL 9	14	8.000	16,000	13.6	73.7	13.91352	150	6.6	3.3	42.2	78.0	5.3	5.8
EEL 10–12	22	4.014	24,000	349.5	68.5	21.87559	169	6.3	2.4	293.2	83.3	3.4	4.0
EEL 14+30	20	4.908	8,000	1.3	64.7	19.91925	235	5.3	2.1	173.5	86.2	2.8	3.4
EEL 15–17	18	3.605	24,000	353.4	65.6	17.90038	171	6.2	2.7	250.2	85.0	3.5	4.3
EEL 18	10	2.299	24,000	9.9	63.0	9.98081	469	3.7	2.2	135.0	81.1	2.8	3.5
EEL 19	17	8.576	16,000	8.6	75.8	16.91480	188	5.9	2.6	23.9	76.4	4.4	4.8
EEL 20–23	43	4.355	24,000	339.4	73.6	42.80025	210	5.6	1.5	323.2	75.1	2.4	2.7
EEL 24	15	6.508	16,000	17.7	63.0	14.96795	437	3.9	1.8	117.6	76.6	2.3	2.9
EEL 26	12	5.959	0	3.1	68.7	11.98352	668	3.1	1.7	58.5	87.6	2.4	2.8
EEL 27	8	7.549	12,000	347.8	63.4	7.97132	244	5.2	3.6	248.2	80.1	4.4	5.6
EEL 28	9	3.388	8,000	344.4	54.8	8.99144	934	2.7	1.7	230.1	71.1	1.7	2.4
EEL 29	11	5.228	24,000	6.6	63.3	10.97825	460	3.8	2.1	146.1	82.9	2.7	3.4
EEL 32	10	1.798	24,000	350.3	49.9	9.97344	339	4.4	2.6	211.1	68.9	2.3	3.5
EEL 33+37	21	9.499	32,000	2.7	81.0	20.94700	377	4.2	1.6	9.4	67.9	3.1	3.2
EEL 34	6	10.887	12,000	2.6	72.3	5.99375	800	2.9	2.4	18.4	82.8	3.7	4.2
EEL 35	8	3.707	12,000	21.2	69.8	7.99215	891	2.7	1.9	75.2	76.6	2.7	3.2
EEL 36	11	5.877	20,000	10.4	66.9	10.97183	355	4.3	2.4	100.5	83.3	3.3	4.0
EEL 38	12	4.931	16,000	344.2	64.8	11.95502	245	5.2	2.8	263.4	78.9	3.6	4.5
EEL 39+40	16	3.631	12,000	346.5	71.5	15.96487	427	3.9	1.8	318.1	80.1	2.7	3.1
EEL 41+42	21	4.146	12,000	347.6	48.2	20.82727	116	7.6	3.0	215.9	66.8	2.5	3.9
EEL 43	11	9.615	12,000	27.7	59.4	10.97817	458	3.8	2.1	114.5	68.2	2.4	3.2
EEL 44+45	15	6.189	12,000	338.0	71.3	14.98382	871	2.8	1.3	308.3	75.8	2.0	2.3
EEL 46	9	9.587	0	0.6	65.1	8.97615	336	4.4	2.8	179.5	86.7	3.7	4.5

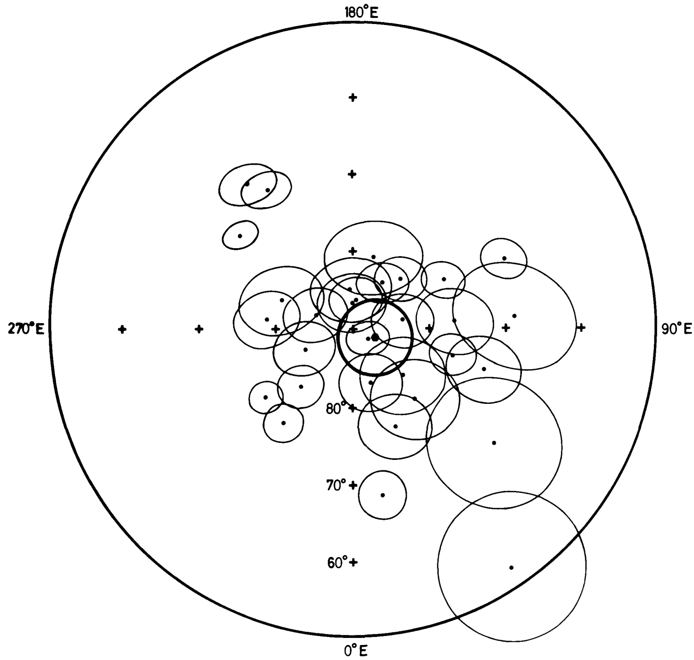

Fig. 5. Mean pole positions (VGP) together with A_{95}-ovals of confidence. The average VGP is indicated by the hexagon

When dealing with palaeosecular variation it is more convenient to use pole positions than directions (Cox, 1962) because the VGPs follow a Fisherian distribution, whereas directions usually follow a non-Fisherian pattern. In Figure 5, the pole positions are plotted together with the ovals of confidence. The pole positions scatter around the north geographic pole with angular separations exceeding rarely 25° to 30°. The distribution appears to be random and can most likely be attributed to palaeosecular variation entirely. Such behaviour could be expected, because the cycles of the non-dipole components ($\approx 10^3$ years) and the dipole wobble ($\approx 10^4$ years) are both shorter than the main volcanic cycle ($6 \cdot 10^5$ years). Averaging all VGPs gives a mean pole at 87.0° N and 69.2° E including with its A_{95}-circle of confidence ($A_{95} = 4.8°$) the north geographic pole. The agreement is significant according to the F-test and is in accord with the hypothesis of an axial dipole.

The distribution of the pole positions around the rotational pole, if uniquely due to palaeosecular variation, should theoretically be Fisherian as pointed out above. In Figure 6 the latitudinal and longitudinal distributions of the pole positions relative to the mean pole and relative to the rotational pole are compared with theoretical distributions. The X^2-test confirms that the longitudinal distribution is significantly ($P > 0.05$) Fisherian in relation to the mean VGP as well as to the geographic pole. As for the latitudinal values, the agreement is only marginally significant ($P < 0.01$). The total number of 31 independent events might be too small to obtain a reliable information from the X^2-test with regard to the longitudinal

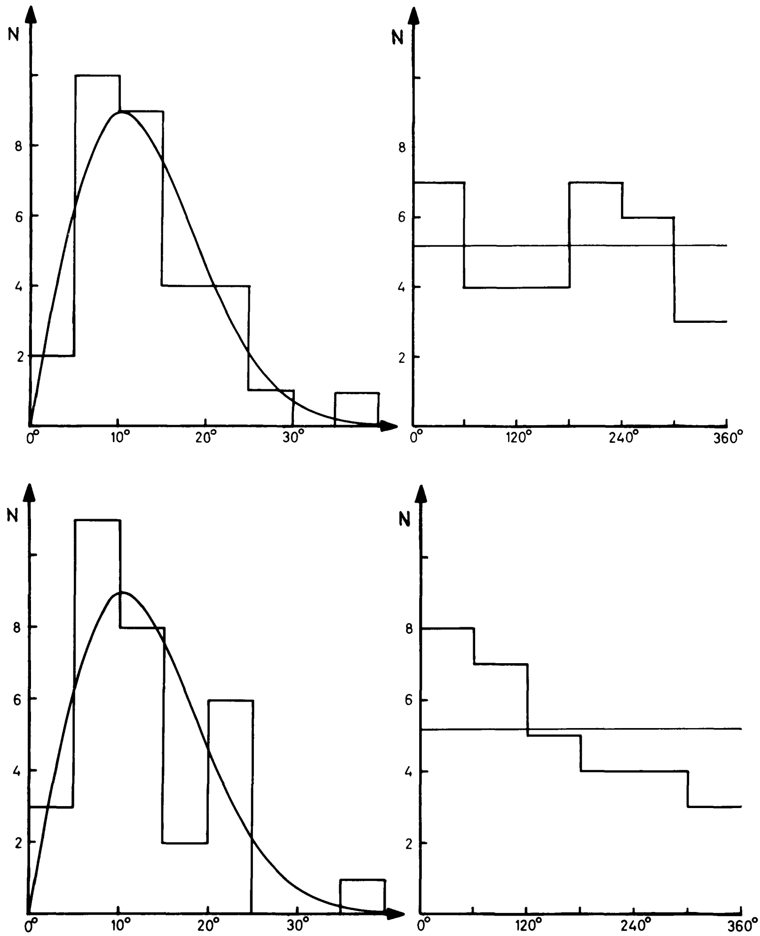

Fig. 6. Latitudinal (*left*) and longitudinal (*right*) distribution of the pole positions (block diagram) compared with the theoretical (Fisherian) distribution in relation to the average VGP (*above*) and the north geographic pole (*below*)

variation (Baag and Helsley, 1974b). Excluding the pole position of the Olbrück lava (EEL 5), located at 52.6° N, 33.9° E, would yield, for instance, significant agreement ($P>0.05$). We may, therefore, assume that the scatter of the pole positions is not in contradiction to a Fisherian distribution.

2. The Angular Dispersion

The quantity of principal interest in the study of palaeosecular variation is the angular dispersion of the VGPs which can be expressed as total standard deviation S_T or Fisher's precision parameter K_T, being related by $S_T^2=2/K_T$; $(K_T=(N-1)/(N-R))$ for small angular dispersions. K is not used because of the

Table 2. Angular dispersion parameters of VGPs. S_T: total standard deviation; S_W: within-site standard deviation; S_B: between-site standard deviation; S_A: standard deviation due to local magnetic anomalies (estimated according to Doell and Cox, 1963); S_F: standard deviation due to the ancient geomagnetic field; S_{Fu} and S_{F1}: upper and lower confidence limits of S_F (tabulated in Cox, 1969). The experimental error and the errors due to tilting are estimated to be 4.1° and 2.6° respectively, both are included in S_W

	S_T	S_W	S_B	S_A	S_F	S_{Fu}	S_{F1}
rel. to mean VGP	15.1°	8.2°	14.9°	1.8°	14.8°	18.0°	12.6°
rel. to geogr. pole	15.4°	8.2°	15.2°	1.8°	15.1°	18.3°	12.8°

approximate nature of this relation. The total standard deviation is computed from:

$$S_T^2 = \frac{1}{(N-1)}\, i\sum \delta_i^2$$

($N=31$: number of independent volcanic events, δ_i = angular separation of the i-th VGP from the mean pole position or from the geographic north pole). S_T^2 comprises the between-site dispersion S_B^2 and the within-site dispersion S_W^2 (Cox, 1969):

$$S_T^2 = S_B^2 + S_W^2/\bar{n}.$$

$\bar{n}(=12.9)$ is the weightened average number of cores per site (Watson and Irving, 1957). S_W^2 is computed from the within-site precision parameter of directions (Watson and Irving, 1957; Cox, 1970). The between-site dispersion results primarily from the ancient secular variation but still includes a small component due to local magnetic anomalies existing when the lava cooled:

$$S_B^2 = S_F^2 + S_A^2$$

(F = ancient field; A = local anomalies). Following Doell's (1972a and b) suggestions and analysis, it is preferable to use S_B and/or S_F which are not affected by the within-site scatter. The quantity S_A is difficult to estimate and usually taken from Doell and Cox (1963). The different dispersion parameters are given in Table 2 together with upper and lower confidence limits (95 % level) of S_F. The differences are small and only apparent in the first decimal.

Figure 7 presents a summary of palaeosecular variation studies carried out by various investigators on volcanics of the Brunhes epoch. The values exhibit a strong latidudinal dependence favouring the models which anticipate such behaviour. The result from the East-Eifel is in excellent agreement with the models, C, E_1, and M as well with the experimental data from comparable latitudes. Doell (1970), for instance, obtained from the investigations of 31 volcanoes in France an angular dispersion $S_F = 15.2°$. Models B, C, and E assume a dipole wobble of 11° whereas curve M is calculated with $S_D = 9°$. Due to the considerable limits of confidence, it cannot be decided from the present experimental data which model is most appropriate to describe the global behaviour of the palaeosecular variation. More data, especially at low and high latitudes are required to obtain reliable informations on the dipole wobble and its relation to the non-dipole field.

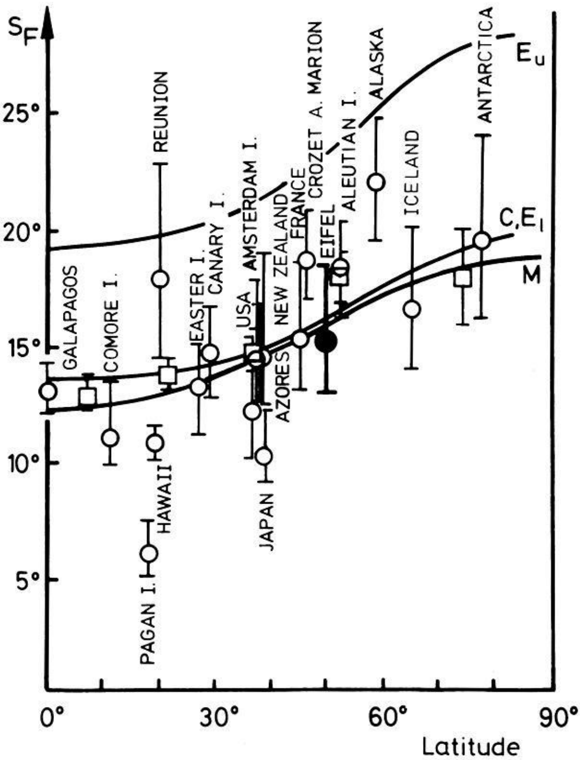

Fig. 7. Angular standard deviation S_F of pole positions with limits of confidence versus latitude on the northern hemisphere (summarised in Isaacson and Heinrichs (1976), and McElhinny and Merrill (1975)). The data of the latter authors (squares) were obtained by averaging VGPs from regions of similar latidues
Dot: East Eifel result. The curves represent models of palaeosecular variation. Models B, C, and E are calculated assuming a dipole wobble $S_D = 11°$ and model M with $S_D = 9°$

Conclusions

Although quite a number of measurements have been carried out to investigate the components and the global behaviour of the palaeosecular variation, there is still some uncertainty about the appropriate regional extent and the length of the time interval necessary to evaluate reasonable coincidence between the average dipole axis and the axis of rotation.

The pole positions determined from the Pleistocene volcanics in the East-Eifel follow a Fisherian distribution about the north geographic pole proving that here both, the time span of about 600,000 years and an area of not more than 20 $\times 24\ km^2$ are sufficient to attain the agreement required by the average dipole hypothesis. This result is not in accord, for instance, with the Pacific data for the same epoch reported by Cox and Doell, (1964) yielding a significant difference between the dipole and rotational axis. Also the assumption that only averaging the VGPs over continental areas (McElhinny and Merrill, 1975) would give sufficient agreement, is not approved by the East-Eifel results. This might be due to the fact, that in this particular case the standing part of the non-dipole field is small or oscillates in periods much shorter than 600,000 years.

Acknowledgement. The authors are indebted to H. Böhnel and R. Giesbert for their assistance during the field and laboratory measurements. The help of Drs. U. Bleil and H.-U. Schmincke (both Ruhr-

Universität Bochum) in selecting the volcanic sites is highly appreciated. The authors further acknowledge the critical comments of U. Bleil and H. Böhnel.

References

Baag, C., Helsley, C.E.: Geomagnetic secular variation model E. J. Geophys. Res. **79**, 4918–4922, 1974a

Baag, C., Helsley, C.E.: Shape analysis of palaeosecular variation data. J. Geophys. Res. **79**, 4923–4932, 1974b

Cox, A.: Analysis of the present geomagnetic field for comparison with palaeomagnetic results. J. Geomag. Geoelectr. **13**, 101–112, 1962

Cox, A.: Confidence limits for the precision parameter k. Geophys. J. **18**, 545–549, 1969

Cox, A.: Latitude dependence of the angular dispersion of the geomagnetic field. Geophys. J. **20**, 253–269, 1970

Cox, A., Doell, R.R.: Long period variations of the geomagnetic field. Bull. Seism. Soc. Am. **54**, 2243–2270, 1964

Creer, K.M.: The dispersion of the geomagnetic field due to secular variation and its determination for remote times from palaeomagnetic data. J. Geophys. Res. **67**, 3461–3476, 1962

Creer, K.M., Irving, E., Nairn, A.E.M.: Palaeomagnetism of the Great Whin Sill. Geophys. J. **2**, 306–323, 1959

Doell, R.R.: Palaeomagnetic secular variation study of lavas from the Massiv Central, France. Earth Planet. Sci. Lett. **8**, 352–362, 1970

Doell, R.R.: Palaeomagnetism of lava flows from Kauai, Hawaii. J. Geophys. Res. **77**, 862–867, 1972a

Doell, R.R.: Palaeomagnetism of volcanic rocks from Niihau, Nihoa and Necker Islands, Hawaii. J. Geophys. Res. **77**, 3725–3730, 1972b

Doell, R.R., Cox, A.: The accuracy of the palaeomagnetic method as evaluated from historic Hawaiian lava flows. J. Geophys. Res. **68**, 1997–2009, 1963

Frechen, J.: Siebengebirge am Rhein, Laacher Vulkangebiet, Maargebiet der Westeifel – Vulkanologisch-petrographische Exkursionen, Sammlung Geologischer Führer, **56**, (3. Auflage). Berlin-Stuttgart: Bornträger 1976

Irving, E., Ward, M.A.: A statistical model of the geomagnetic field. Pure Appl. Geophys. **57**, 47–52, 1964

Isaacson, L.B., Heinrichs, D.F.: Palaeomagnetism and secular variation of Easter Island basalts. J. Geophys. Res. **81**, 1476–1482, 1976

McElhinny, M.W., Merrill, R.T.: Geomagnetic secular variation over the past 5 m.y. Rev. Geophys. Space Phys. **13**, 687–708, 1975

Symons, D.T.A., Stupavsky, M.: A rational palaeomagnetic stability index. J. Geophys. Res. **79**, 1718–1720, 1974

Watson, G.S., Irving, E.: Statistical methods in rock magnetism, Monthly Notices Roy. Astron. Soc., Geophys. Suppl. **7**, 289–300, 1957

Yukutake, T., Tachinaka, H.: Separation of the earth magnetic field into drifting and standing parts, Bull. Earthq. Res. Inst. **47**, 65–97, 1969

Received March 29, 1978 / Revised Version May 12, 1978